Journal of Electrical Engineering, Vol. 74, No. 4, 2023, pp. 311-320

sciendo

PAPER

Throughput performance optimization of NOMA-assisted cooperative relay system with realistic impairments

P. Bachan, Aasheesh Shukla and Atul Bansal

This work aims to investigate the outage and throughput performance of non-orthogonal multiple access assisted cooperative relay system (CRS-NOMA) considering the realistic impairments caused due to in-phase and quadrature-phase imbalance (IQI), channel estimation errors (CEE), and successive interference cancellation (SIC) errors. More specifically, we investigate a model in which two-phase downlink transmission is carried out in two different modes: (i) CRS-NOMA without direct links and (ii) CRS-NOMA with direct links (CRS-DLNOMA). In CRS-NOMA mode, the source broadcasts a composite NOMA signal to destination users with the assistance of a decode-and-forward (DF) relay. In contrast, in CRS-DLNOMA, direct and cooperative links are available for transmission. We derive the analytical expressions of outage probability and throughput for both the NOMA destinations to evaluate the system performance of both CRS-NOMA and CRS-DLNOMA modes of transmission. Furthermore, numerical simulations also study and validate the influence of IQI, CEE, and SIC errors on the outage and throughput performance. The simulation results verify that realistic impairments degrade the system performance, but the presence of direct link has a positive impact on outage and throughput. Additionally, we use the golden search method to optimize the power allocation factor (PAF) and transmission rate to maximize the throughput at the near user while ensuring the throughput constraint at the far user.

Keywords: Channel estimation error, in-phase and quadrature-phase imbalance, non-orthogonal multiple access, outage probability, successive interference cancellation, and throughput

1. Introduction

Non-orthogonal multiple access (NOMA) has been considered an appropriate contender in beyond fifth-generation (B5G) networks to provide services with ultra-high data rate, superior spectral efficiency (SE), low bit error probability, and superior quality of service [1]. In practical scenarios where source-to-destination separations are relatively large, relay-assisted NOMA, known as NOMA-assisted cooperative relay system (CRS-NOMA), is employed to enable the convergence of a heterogeneous network [2]. In the CRS-NOMA system, the source broadcasts the composite NOMA signal to the relay in phase-I, which decodes and retransmits the signal to both the users in the second phase. At the destination, maximum likelihood detection (MLD) is utilized, in which the signal with the higher power allocation factor (PAF) is decoded first by considering other users' signals as interference, which is followed by the SIC process to detect the signal with low PAF [3].

In recent literature, cooperative NOMA has been well investigated regarding outage probability and throughput [4-6]. It is proven that in a perfect scenario, this scheme perfectly outperforms the other multiple access techniques. However, there is a large impact of realistic impairments, such as in-phase and quadrature-phase imbalance (IQI), channel estimation errors (CEE), and SIC errors, on the performance of the CNOMA system [7,8]. Therefore, the investigation of the CRS-NOMA network under the scenario of realistic impairments is crucial and examined by the research community [9]. To the best of our knowledge, in almost all literature collective impact of CEE and SIC error is only investigated on the performance of the CRS-NOMA system. In [10], the effect of the residual interference signal and channel error on the outage performance of the CRS-NOMA system was examined. The impact of impairments was observed to be significant in the extensive signal-to-noise ratio (SNR) regime. An AF relay-assisted NOMA system was proposed in [11], in which SIC and maximum-ratio combining (MRC) techniques were applied twice at the receiver to improve the diversity performance. To improve the outage performance of channel error-limited downlink NOMA transmission, the selection diversity scheme is studied in [12]. An underlay CR-NOMA system was studied in [13] to evaluate the efficacy of all hardware impairments on the outage probability of the system. In this study, an optimal PAF algorithm was also proposed to deliver improved fairness to both the users in the network. An outage-based optimization algorithm for the uplink NOMA system was examined in [14], where the impact of SIC error propagation on outage performance is evaluated. The performance of AF relay-assisted overlay CR-NOMA has been analyzed in [15], where both perfect and imperfect SIC and CEE scenarios are considered to evaluate the outage probability of primary and secondary users. In [16], a CNOMA-IoT network with a direct link is studied, in which throughput and goodput expressions were derived to evaluate the performance in the presence of

Department of Electronics and Communication Engineering, GLA University, Mathura, Uttar Pradesh, India
p.bachan@gla.ac.in, aasheesh.shukla@gla.ac.in, atul.bansal@gla.ac.in

https://doi.org/10.2478/jee-2023-0038, Print (till 2015) ISSN 1335-3632, On-line ISSN 1339-309X

SIC error and CEE. The results show maximum throughput is attained by adjusting the relay and source power. A virtual MIMO-based CNOMA system is investigated in [17], and overall error performance is evaluated by considering imperfect SIC and CEE scenarios. In this system, the selective relay method is utilized to achieve the diversity benefit at the receiver. A full-duplex NOMA model with MRC is studied in [18], where the overall achievable rate at far user is improved.

Moreover, besides SIC error and CEE, a communication system's overall performance is limited due to distortion noise, such as in-phase and quadrature-phase imbalance (IQI) [19]. This distortion noise arises in transceiver hardware due to amplitude and phase mismatch resulting in image frequency signal impairments [20]. The impact of RF imperfection in single and multicarrier wireless transceivers was studied in [21]. This study provides a detailed analysis of IQI evaluation and compensation techniques that can be utilized in emerging technologies. In [22], a multicarrier NOMA technique under a severe fading environment was studied. The results showed that the outage of higher-order users is more affected due to distortion noise. An optimal throughput and outage performance of a multi-relay NOMA network is examined in [23], where the impact of residual hardware impairments (RHI) and the availability of direct links were analyzed. A NOMA system for backscatter communication was investigated in [24] to evaluate the reliability of the communication system in an imperfect scenario. It was shown that compared to RHI, phase noise (PN) has a more severe effect on reliability performance. The work in [25] shows that PN significantly impacts both users' NOMA system error performance. It was examined that the IQI factor directly depends on PAF and diversity order. In [26], an optimal receiver design technique is proposed that can resist the effect of IQI on transmission reliability and error performance. It was demonstrated that PAF has the most significant effect on IQI, which may lead to degradation in system performance.

Most of the investigated work on CRS-NOMA systems examined the performance in perfect or imperfect SIC scenarios. None of these works exploits the benefit of enhanced performance by considering the direct path along with cooperative transmission to NOMA destinations. Furthermore, the throughput performance of CRS-NOMA systems is examined by very few works in the presence of either SIC or IQI or CEE error.

To the best of our knowledge, no prior research has exhaustively investigated CRS-NOMA systems with all realistic impairments. Therefore, this work studies the outage and throughput performance of the cooperative relay-based NOMA system in the presence of all realistic impairments considering two different modes of transmission: CRS-NOMA and CRS-DLNOMA.

The significant contributions of this investigation are as follows:

- A NOMA-assisted cooperative relay system for downlink transmission is investigated, where realistic imperfections of IQI, CEE, and SIC error are considered.
- We derive analytical expressions of an end-to-end outage and throughput of the CRS-NOMA model for both users considering all the realistic impairments.
- The performance analysis of the cooperative NOMA system is extended for two different modes of transmission such as CRS-NOMA and CRS-DLNOMA.
- We propose an efficient golden search-based algorithm for optimizing the PAF and transmission rate. The optimal values of PAF and rate are utilized to maximize the overall system throughput.
- Numerical simulations are performed to validate the derived mathematical expressions. Furthermore, valuable insights are drawn by comparing the transmission modes' results in the presence and absence of IQI, CEE, and SIC errors.

The remainder of this article is structured as follows: Section 2 presents the signal description for the DF relay-assisted NOMA Network considering CRS-NOMA and CRS-DLNOMA modes of transmission. Based on the signal-to-interference-plus-noise ratio (SINR) expressions derived in Section 2, the analytical expressions of end-to-end outage probability and throughput are derived in Section 3 and Section 4, respectively. In Section 5, we propose an algorithm for optimizing the system's power allocation factor and transmission rate, so as to improve the system throughput. The numerical simulation-based results of both performance metrics are provided in Section 6. The insightful conclusions related to the impact of realistic impairments on the performance of the investigated scheme are presented in Section 7.

2. System model

We consider a DF relay-assisted CNOMA network for downlink transmission as depicted in Fig. 1. In this model, two phases of downlink transmission are carried out in two different modes: (i) Cooperative transmission without a direct link (CRS-NOMA) and (ii) Cooperative transmission with a direct link (CRS-DLNOMA). In CRS-NOMA mode, the source (S) broadcasts a composite NOMA signal to both users with the assistance of a DF relay. In CRS-DLNOMA, S broadcasts composite NOMA signals to users via direct and cooperative links. The users then combine the signals received through both links using the MRC technique.

As depicted in Fig. 1, all the wireless links are modelled by Rayleigh fading-based channel coefficients. These coefficients are modelled by $h_{AB} \sim \mathcal{CN}(0, \lambda_{AB})$ where, $\{A, B\} \in \{S, R, U_i\}$, $i = n, f$, $A \neq B$. The average channel gain is modelled as $\lambda_{AB} = d_{AB}^{-\beta}$ where d_{AB} length of hop link between nodes A and B, and β is the path loss exponent. Due to practical limitations, channel estimation errors (CEE) are experienced by each node during the transmission. So, considering CEE (e), we estimate the channel coefficients as $\tilde{h}_{AB} = h_{AB} - e$, where e is modelled as $e \sim \mathcal{CN}(0, \lambda_e)$. Apart from CEE, we also consider the distortion due to IQI between nodes $S \rightarrow U_i$, $S \rightarrow R$, and $R \rightarrow U_i$ denoted as η_{SU_i}, η_{SR}, and η_{RU_i} respectively, where η_{SU_i}, η_{SR}, and η_{RU_i} are modelled as $\mathcal{CN}(0, Pk^2)$ with k^2 being the IQI impairment coefficient considered to be the same at transmitter and receiver, and P denotes the power, which is assumed to be equal at all nodes.

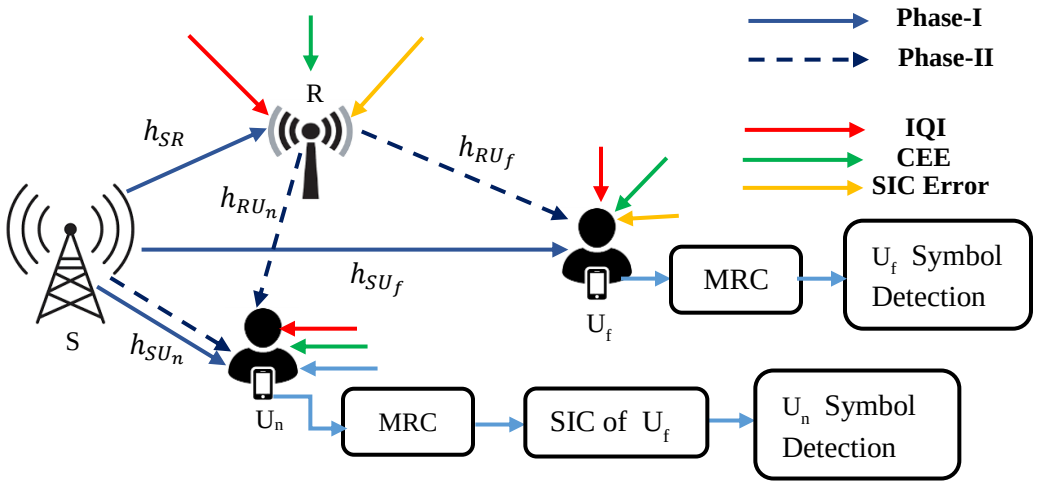

Fig. 1. A two-phase NOMA-assisted cooperative relay system with realistic impairments.

In this model, the overall downlink transmission is carried out in two phases using two different modes of communication: CRS-NOMA and CRS-DLNOMA. Firstly, S broadcasts the combined NOMA signal to relay both the users simultaneously, which is given by,

$$S = \sqrt{P\mu_n}x^1_{U_n} + \sqrt{P\mu_f}x^1_{U_f}, \quad (1)$$

where $x^1_{U_n}$ and $x^1_{U_f}$ represent the signals corresponding to the near user U_n and far user U_f respectively, P is the transmit signal power at S, μ_n, and μ_f are the assigned PAF to U_n and U_f based on the distance and signal strength.

The signals received by U_n, U_f, and R are given, respectively as

$$y^1_{SU_n} = h_{SU_n}\left(\sqrt{P\mu_n}x^1_{U_n} + \sqrt{P\mu_f}x^1_{U_f} + \eta_{SU_n}\right) + n_{U_n}, \quad (2)$$

$$y^1_{SU_f} = h_{SU_f}\left(\sqrt{P\mu_n}x^1_{U_n} + \sqrt{P\mu_f}x^1_{U_f} + \eta_{SU_f}\right) + n_{U_f}, \quad (3)$$

$$y^1_{SR} = h_{SR}\left(\sqrt{P\mu_n}x^1_{U_n} + \sqrt{P\mu_f}x^1_{U_f} + \eta_{SR}\right) + n_R, \quad (4)$$

where η_{SU_n}, η_{SU_f}, and η_{SR} are distortion noise due to IQI error produced during the transmission from $S \to U_n$, $S \to U_f$, and $S \to R$ respectively. All the distortion noises are modelled as $\eta_{Si} \sim \mathcal{CN}(0, Pk^2_{Si})$, where $k^2_{Si} = k^2$, $i \in \{U_n, U_f, R\}$, is the IQI factor at different nodes. We assume $n_{U_n} = n_{U_f} = n_R = n$ is the additive white Gaussian noise (AWGN) modelled by $n \sim \mathcal{CN}(0, N_0/2)$.

Based on the CNOMA transmission scheme in phase-I, $x^1_{U_f}$ is decoded at U_f, U_n, and R, which is followed by the SIC process to decode $x^1_{U_n}$ at U_n. The corresponding received SINRs are given respectively,

$$\Omega^{x^1_{U_f}}_{SU_f} = \frac{\mu_f P\tilde{\lambda}_{SU_f}}{P\tilde{\lambda}_{SU_f}(\mu_n+k^2)+P\lambda_e(1+k^2)+N_0/2}, \quad (5)$$

$$\Omega^{x^1_{U_f}}_{SU_n} = \frac{\mu_f P\tilde{\lambda}_{SU_n}}{P\tilde{\lambda}_{SU_n}(\mu_n+k^2)+P\lambda_e(1+k^2)+N_0/2}, \quad (6)$$

$$\Omega^{x^1_{U_f}}_{SR} = \frac{\mu_f P\tilde{\lambda}_{SR}}{P\tilde{\lambda}_{SR}(\mu_n+k^2)+P\lambda_e(1+k^2)+N_0/2}, \quad (7)$$

$$\Omega^{x^1_{U_n}}_{SU_n} = \frac{\mu_n P\tilde{\lambda}_{SU_n}}{\delta P\tilde{\lambda}_{SU_n}(\mu_f+k^2)+P\lambda_e(1+k^2)+N_0/2}, \quad (8)$$

where δ is the level of SIC error occurred during detection of $x^1_{U_n}$ at U_n.

In phase-II, R retransmits the superimposed signal to both the users, and MRC is performed at the destination user to combine the signals received in phase-I and phase-II. The signals received by U_n and U_f are given respectively as

$$y^2_{RU_n} = h_{RU_n}\left(\sqrt{P\mu_n}\tilde{x}^1_{U_n} + \sqrt{P\mu_f}\tilde{x}^1_{U_f} + \eta_{RU_n}\right) + n_{U_n}, \quad (9)$$

$$y^2_{RU_f} = h_{RU_f}\left(\sqrt{P\mu_n}\tilde{x}^1_{U_n} + \sqrt{P\mu_f}\tilde{x}^1_{U_f} + \eta_{RU_f}\right) + n_{U_f}. \quad (10)$$

Based on the received signal in (9) and (10), the corresponding received SINRs for detecting $x^2_{U_f}$ and $x^2_{U_n}$ in phase-II are given respectively as

$$\Omega^{x^2_{U_f}}_{RU_f} = \frac{\mu_f P\tilde{\lambda}_{RU_f}}{P\tilde{\lambda}_{RU_f}(\mu_n+k^2)+P\lambda_e(1+k^2)+N_0/2},$$

$$\Omega^{x^2_{U_f}}_{RU_n} = \frac{\mu_f P\tilde{\lambda}_{RU_n}}{P\tilde{\lambda}_{RU_n}(\mu_n+k^2)+P\lambda_e(1+k^2)+N_0/2},$$

$$\Omega^{x^2_{U_n}}_{RU_n} = \frac{\mu_n P\tilde{\lambda}_{RU_n}}{P\tilde{\lambda}_{SU_n}(\delta\mu_f+k^2)+P\lambda_e(1+k^2)+N_0/2}.$$

For CRS-NOMA, as direct links are unavailable, users decode their signals only in the second phase of the transmission. However, for CRS-DLNOMA, both direct and cooperative links are available so that users decode their signals in both stages. Thus, by employing MRC in phase-II, the SINRs for the detection of $x_{U_f}^2$ and $x_{U_n}^2$ are given respectively as,

$$\Omega_{f\_CTDL-NOMA}^{x_{U_f}^1} = \Omega_{SU_f}^{x_{U_f}^1} + \Omega_{RU_f}^{x_{U_f}^2}, \quad (11)$$

$$\Omega_{n\_CTDL-NOMA}^{x_{U_f}^1} = \Omega_{SU_n}^{x_{U_f}^1} + \Omega_{RU_n}^{x_{U_f}^2}, \quad (12)$$

$$\Omega_{n\_CTDL-NOMA}^{x_{U_n}^1} = \Omega_{SU_n}^{x_{U_n}^1} + \Omega_{RU_n}^{x_{U_n}^2}. \quad (13)$$

3. Outage analysis at NOMA destinations

This section provides the analytical expressions of outage probability for NOMA users considering CRS-NOMA and CRS-DLNOMA modes of transmission. To simplify the analysis, we consider the target SINR threshold, $\Omega_{th_n} = \Omega_{th_f} = \Omega_{th}$.

3.1 Overall outage probability of CRS-NOMA

Based on the CRS-NOMA transmission scheme, an outage event at U_i occurs if the instantaneous SINR of the received signal falls below the threshold Ω_{th}. Therefore, the probability of an outage at U_i for CRS-NOMA mode is expressed as,

$$OP_{CRS-NOMA}^{e2e_{U_i}} = 1 - Pr\left(\Omega_{SR}^{x_{U_i}} > \Omega_{th_i}\right) Pr\left(\Omega_{RU_i}^{x_{U_i}} > \Omega_{th_i}\right), \quad i \in \{n, f\}, \quad (14)$$

where $\Omega_{th_i} = 2^{lR_i} - 1$ is the threshold SINR of the user with R_i and l being the desired data rate of the user in bits/s/Hz and the number of phases in the transmission scheme, respectively.

The outage probability of x_{U_f} at R and U_f is expressed as,

$$Pr\left(\Omega_j^{x_{U_f}} > \Omega_{th_f}\right) = exp\left(-\Omega_{th_f}\gamma_j^{x_{U_f}}\right),\ j \in \{SR, SU_f, RU_f\} \quad (15)$$

where $\gamma_j^{x_{U_f}} = \frac{\left(P\lambda_e + P\lambda_e k_j^2 + N_0/2\right)}{\theta_j\left(P\mu_f - P\mu_n\Omega_{th_f} - Pk_j^2\Omega_{th_f}\right)}$, and

$\theta_j = E\left[\left|h_j\right|^2\right] - E[|e|^2]$.

By substituting (15) in (14), we get the overall outage at U_f. Similarly, the outage probability of x_{U_n} at R and U_n is expressed as,

$$Pr\left(\Omega_z^{x_{U_n}} > \Omega_{th_n}\right) = exp\left(-\Omega_{th_n}\gamma_z^{x_{U_n}}\right)exp\left(-\Omega_{th_f}\gamma_z^{x_{U_f}}\right), \quad z \in \{SR, SU_n, RU_n\} \quad (16)$$

where $\gamma_z^{x_{U_n}} = \frac{\left(P\lambda_e + P\lambda_e k_z^2 + N_0/2\right)}{\theta_z\left(P\mu_n - \delta P\mu_f\Omega_{th_n} - Pk_z^2\Omega_{th_n}\right)}$,

$\gamma_z^{x_{U_f}} = \frac{\left(P\lambda_e + P\lambda_e k_z^2 + N_0/2\right)}{\theta_z\left(P\mu_f - P\mu_n\Omega_{th_f} - Pk_z^2\Omega_{th_f}\right)}$, and

$\theta_z = E[|h_z|^2] - E[|e|^2]$.

By substituting (16) in (14), we get the overall outage at U_n.

3.2 Overall outage probability of CRS-DLNOMA

In CRS-DLNOMA, direct links are also available for transmission from $S \to U_i$. Thus, the signals are received by the user in both phases. Finally, to achieve reception diversity, both the variants of the signals are combined at U_i using the MRC process.

The overall outage probability of U_f for CRS-DLNOMA is expressed as,

$$OP_{CRS-DLNOMA}^{e2e\_U_f} = Pr\left(\Omega_{SR}^{x_{U_f}} > \Omega_{th_f}\right) Pr\left(\Omega_{CRS-NOMA}^{x_{U_f}} < \Omega_{th_f}\right) + \left(1 - \Pr\left(\Omega_{SR}^{x_{U_f}} > \Omega_{th_f}\right)\right)\left(1 - \Pr\left(\Omega_{SU_f}^{x_{U_f}} > \Omega_{th_f}\right)\right), \quad (17)$$

where $Pr\left(\Omega_{CRS-NOMA}^{x_{U_f}} < \Omega_{th_f}\right)$ is dependent on the CDF of two independent SINRs $\Omega_{RU_f}^{x_{U_f}}$ and $\Omega_{SU_f}^{x_{U_f}}$, which is expressed as,

$$Pr\left(\Omega_{CRS-NOMA}^{x_{U_f}} < \Omega_{th_f}\right) = 1 - \left[\emptyset_{SR_{U_f}}^{x_{U_f}} \exp\left(-\Omega_{th_f}\gamma_{SU_f}^{x_{U_f}}\right) + \emptyset_{RS_{U_f}}^{x_{U_f}} \exp\left(-\Omega_{th_f}\gamma_{RU_f}^{x_{U_f}}\right)\right], \quad (18)$$

where $\emptyset_{SR_{U_f}}^{x_{U_f}} = \gamma_{SU_f}^{x_{U_f}} / \left(\gamma_{SU_f}^{x_{U_f}} - \gamma_{RU_f}^{x_{U_f}}\right)$,

and $\emptyset_{RS_{U_f}}^{x_{U_f}} = \gamma_{RU_f}^{x_{U_f}} / \left(\gamma_{RU_f}^{x_{U_f}} - \gamma_{SU_f}^{x_{U_f}}\right)$.

By substituting probability expressions obtained in (15) and (18) in (17), we get the overall outage at U_f.

The overall outage probability of U_n for CRS-DLNOMA is expressed as

$$OP_{CRS-DLNOMA}^{e2e_{U_n}} = OP_{n_{CRS-DLNOMA}}^{x_{U_f}} + \left(1 - OP_{n_{CRS-DLNOMA}}^{x_{U_f}}\right) \times OP_{CRS-DLNOMA}^{x_{U_n}}, \quad (19)$$

where $OP_{n\_CRS-DLNOMA}^{x_{U_f}}$ is the OP of x_{U_f} detected at U_n using MRC and $OP_{CRS-DLNOMA}^{x_{U_n}}$ is the OP of x_{U_n} detected at U_n, which are expressed respectively as,

$$OP_{n_{CRS-DLNOMA}}^{x_{U_f}} = exp\left(-\Omega_{th_f}\gamma_{SR}^{x_{U_f}}\right) \times \left(1 - \left[\emptyset_{SR_{U_n}}^{x_{U_f}} \exp\left(-\Omega_{th_f}\gamma_{SU_n}^{x_{U_f}}\right) + \emptyset_{RS_{U_n}}^{x_{U_f}} \exp\left(-\Omega_{th_f}\gamma_{RU_n}^{x_{U_f}}\right)\right]\right) + \left(1 - exp\left(-\Omega_{th_f}\gamma_{SR}^{x_{U_f}}\right)\right)\left(1 - exp\left(-\Omega_{th_f}\gamma_{SU_n}^{x_{U_f}}\right)\right), \quad (20)$$

where $\emptyset_{SR_{U_n}}^{x_{U_f}} = \gamma_{SU_n}^{x_{U_f}} / \left(\gamma_{SU_n}^{x_{U_f}} - \gamma_{RU_n}^{x_{U_f}}\right)$,

$\emptyset_{RS_{U_n}}^{x_{U_f}} = \gamma_{RU_n}^{x_{U_f}} / \left(\gamma_{RU_n}^{x_{U_f}} - \gamma_{SU_n}^{x_{U_f}}\right)$,

and

$$OP_{CRS-DLNOMA}^{x_{U_n}} = exp\left(-\Omega_{th_n}\gamma_{SR}^{x_{U_n}}\right) \times \left(1 - \left[\emptyset_{SR_{U_n}}^{x_{U_n}} \exp\left(-\Omega_{th_n}\gamma_{SU_n}^{x_{U_n}}\right) + \emptyset_{RS_{U_n}}^{x_{U_n}} \exp\left(-\Omega_{th_n}\gamma_{RU_n}^{x_{U_n}}\right)\right]\right) + \left(1 - exp\left(-\Omega_{th_n}\gamma_{SR}^{x_{U_n}}\right)\right)\left(1 - exp\left(-\Omega_{th_n}\gamma_{SU_n}^{x_{U_n}}\right)\right). \quad (21)$$

By substituting probability expressions obtained in (20) and (21) in (19), we get the overall outage at U_n.

4. Overall throughput analysis

In order to decode its own symbol, the near user must first decode the symbol used by the far user by employing the SIC technique. So if SIC is not perfect, then this results in performance degradation in terms of link reliability and throughput. For this reason, it makes sense to maximize near-user throughput while ensuring the desired far-user throughput. In terms of bits per channel use (bpcu), the far user and near user throughput is described as

$$\tau^{U_i} = \frac{1}{2}R_i(1 - OP^{U_i}),\ i \in \{n, f\} \quad (22)$$

where R_i and OP^{U_i} are the desired transmission rate and outage probability of the i[th] user, respectively.

By substituting the outage probability expressions obtained for CRS-NOMA ((15) and (16)) and CRS-DLNOMA ((17) and (19)) in (22), we get the throughput of both the users in the network.

Finally, the overall throughput of CRS-NOMA and CRS-DLNOMA is expressed as,

$$\tau_{overall} = R_n(1 - OP^{U_n}) + R_f\left(1 - OP^{U_f}\right). \quad (23)$$

5. Throughput performance optimization

In this section, we define the optimization problem for the overall throughput performance of CRS-NOMA and propose an algorithm for optimizing the system's power allocation factor and transmission rate.

The objective of this optimization is to attain the maximum overall throughput of the CRS-NOMA scheme with a constraint on minimal desirable throughput τ_d for the far user U_f. In particular, we optimize the PAF and transmission rate to maximize the throughput at $U_n$while ensuring the throughput constraint at U_f. The optimization problem can be formulated as

$$\max_{R_f, R_f, \mu_f, \mu_n} \tau^{U_n}$$
$$s.t.\ \ \mu_f + \mu_n = 1, \text{and } \tau^{U_f} \geq \tau_d \quad (24)$$

To satisfy the optimization objective defined in (24), we examine the PAF and desired rate of the user considering a realistic impairment scenario. Due to the complex design of transmitters and receivers, it is difficult to determine the exact error value due to imperfect SIC. Thus, we consider the SIC failure for optimal throughput performance. The analysis of throughput optimization is provided as follows:

Based on the NOMA transmission scheme, U_f directly decodes its own information, and SIC is not performed during the decoding process. Thus, SIC failure is only possible during the detection of x_{U_n} at U_n when x_{U_f} is not perfectly removed from the composite signal. Therefore, the corresponding SINRs for the successful detection of x_{U_n} at U_n in perfect SIC scenario for phase-I and phase-II are given respectively as

$$\check{\Omega}_{SU_n}^{x_{U_n}^1} = \frac{\mu_n P\tilde{\lambda}_{SU_n}}{P\lambda_e(1+k^2)+N_0/2}\ , \quad (25)$$

$$\check{\Omega}_{RU_n}^{x_{U_n}^2} = \frac{\mu_n P\tilde{\lambda}_{RU_n}}{k^2 P\tilde{\lambda}_{SU_n}+P\lambda_e(1+k^2)+N_0/2}\ , \quad (26)$$

In the case of SIC failure, the corresponding SINRs for the successful detection of x_{U_n} at U_n for phase-I and phase-II are given, respectively as

$$\hat{\Omega}_{SU_n}^{x_{U_n}^1} = \frac{\mu_n P\tilde{\lambda}_{SU_n}}{P\tilde{\lambda}_{SU_n}(\mu_f+k^2)+P\lambda_e(1+k^2)+N_0/2}, \quad (27)$$

$$\hat{\Omega}_{RU_n}^{x_{U_n}^2} = \frac{\mu_n P\tilde{\lambda}_{RU_n}}{P\tilde{\lambda}_{SU_n}(\delta\mu_f+k^2)+P\lambda_e(1+k^2)+N_0/2}. \quad (28)$$

By substituting the updated SINR expressions obtained in (25), (26), (27) and (28) in (14) and (19), we get the corresponding outage probability of U_n for CRS-NOMA and CRS-DLNOMA, respectively.

Finally, by substituting the updated expression of OP^{U_n} in (23), we get the throughput of U_n.

Algorithm 1 Throughput Optimization Algorithm for CRS-NOMA

Initialization: Initialize the following set of parameters:
- τ_d : Minimal desirable throughput for the far user U_f
- $\mu_f = 0.5{:}\,\vartheta : 1$, ϑ is the step size of PAF μ_f
- R'_f: Initial value of R_f
- a, b: Tolerance error of R_f, R_n
- Initial value of R_n^{min} and R_n^{max}
- $\tau_{max}^{U_n} = 0$
- $\nabla = 0.5(\sqrt{5} - 1)$: Step size of golden search method

for $i = 1 : length(\mu_f)$ **do**
  $R_f \leftarrow \tau\left(R'_f, \mu_f(i)\right)$
  while $\left|R'_f - R_f\right| \leq a$ **do**
    $R'_f \leftarrow \tau\left(R_f, \mu_f(i)\right)$
  end while
  $R_f \leftarrow R'_f$
  / / golden search method for R_n
  $R_n^1 = R_n^{max} - (R_n^{max} - R_n^{min})\nabla$
  $R_n^2 = R_n^{max} + (R_n^{max} - R_n^{min})\nabla$
  while $\left|R_n^{max} - R_n^{min}\right| \leq b$ **do**
    $\tau_1^{U_n} \leftarrow \tau^{U_n}(R_n^1)$
    $\tau_2^{U_n} \leftarrow \tau^{U_n}(R_n^2)$

if $\tau_1^{U_n} > \tau_2^{U_n}$
$R_n^{max} \leftarrow R_n^2$
else
$R_n^{min} \leftarrow R_n^1$
end if
end while
$R_n \leftarrow (R_n^{max} + R_n^{min})/2$
$\tau_{temp}^{U_n} \leftarrow \tau^{U_n}(R_n)$
if $\tau_{temp}^{U_n} > \tau_{max}^{U_n}$
$\tau_{max}^{U_n} \leftarrow \tau_{temp}^{U_n}$
$R_f^{opt} \leftarrow R_f$
$R_n^{opt} \leftarrow R_n$
$\mu_f^{opt} \leftarrow \mu_f(i)$
$\mu_n^{opt} \leftarrow 1 - \mu_f^{opt}$
end if
end for

Output: $\mu_f^{opt}, \mu_n^{opt}, R_f^{opt}, R_n^{opt}$

In the CRS-NOMA transmission, total power is entirely distributed between U_f and U_n. According to (14) and (22), τ^{U_f} is a growing function of μ_f, whereas τ^{U_n} is not a growing function of μ_n both in the presence and absence of SIC error. Thus, an optimal power allocation strategy is required to address this problem. The steps for optimal throughput design of the CRS-NOMA scheme are as follows:

Step I: Determine R_f for all possible μ_f such that $\mu_f + \mu_n = 1$ and $\tau^{U_f}(R_f) = \tau_d$.

$$R_f := \tau(R_f) = \frac{\tau_d}{1 - OP^{U_f}}, \tag{29}$$

Step II: For the feasible value of μ_f, μ_n and derived the value of R_f, determine the value of R_n.

Let $\check{R}$ and $\hat{R}$ be the transmission rate corresponding to the SINRs under perfect and imperfect SIC scenarios mentioned in (26) and (28). Then the optimal value of R_n that maximizes τ^{U_n} is expressed as,

$$R_n^{opt} = \begin{cases} R_n'^{max}, & 0 \le R_n \le \hat{R} \\ R_n''^{max}, & \hat{R} \le R_n \le \check{R} \end{cases}, \tag{30}$$

where $\hat{R} = \frac{1}{2} log_2\left(1 + \hat{\Omega}_{RU_n}^{x_{U_n}^2}\right)$, $\check{R} = \frac{1}{2} log_2\left(1 + \check{\Omega}_{RU_n}^{x_{U_n}^2}\right)$. $R_n'^{max}$ and $R_n''^{max}$ are the optimal rates at which τ^{U_n} attains its maximum value under SIC failure and perfect SIC, respectively. We use the golden search method to find the value of $R_n'^{max}$ and $R_n''^{max}$.

Step III: Utilize optimal PAF strategy to determine the optimal throughput at U_n.

Using the one-dimensional numerical search approach, we identify the set of effective PAF values of μ_f such that $0.5 \le \mu_f \le 1$. Step I leads to the value of R_f and utilizing the value of $\mu_n = 1 - \mu_f$ in Step II R_n is obtained. These iterations are continuously repeated until we attain an optimal μ_n at which maximum throughput at U_n is identified. Finally, we obtain the set of optimal values of PAF and transmission rates for both users. The proposed algorithm for optimizing the throughput performance of the CRS-NOMA scheme is provided in Algorithm 1.

6. Numerical results and discussions

In this section, we present the simulation-based results to evaluate the impact of IQI, CEE, and SIC errors on the performance of the CRS-NOMA network. Furthermore, based on analytical expressions, end-to-end outage probability and throughput results are analyzed for both CRS-NOMA and CRS-DLNOMA to draw the insightful influence of direct links on the system performance. The critical system parameters and notations set for the investigated model are listed in Table 1.

Table 1. Notations and simulation parameters

Parameters	Values
Samples for channel realization	10^5
Desired data rate of $\boldsymbol{R_n}$	1 bits/s/Hz
Desired data rate of $\boldsymbol{R_f}$	0.5 bits/s/Hz
SINR threshold, $\boldsymbol{\Omega_{th}}$	$2^{2R} - 1$
Power allocation Factors, μ_f, μ_n	0.8, 0.2
Link distances in meters $\boldsymbol{d_{SR}}$ $\boldsymbol{d_{SU_f}}$, $\boldsymbol{d_{SU_n}}$, $\boldsymbol{d_{RU_f}}$, $\boldsymbol{d_{RU_n}}$	1m, 4m, 2m, 3m, 1m
IQI factor, $\boldsymbol{k}$	0.25
CEE, $\boldsymbol{\lambda_e}$	0.008
SIC error, $\boldsymbol{\delta}$	0.001
Average channel gain of each link, $\boldsymbol{\lambda_{AB}}$	$d_{AB}^{-\beta}$
Path loss exponent, $\boldsymbol{\beta}$	2

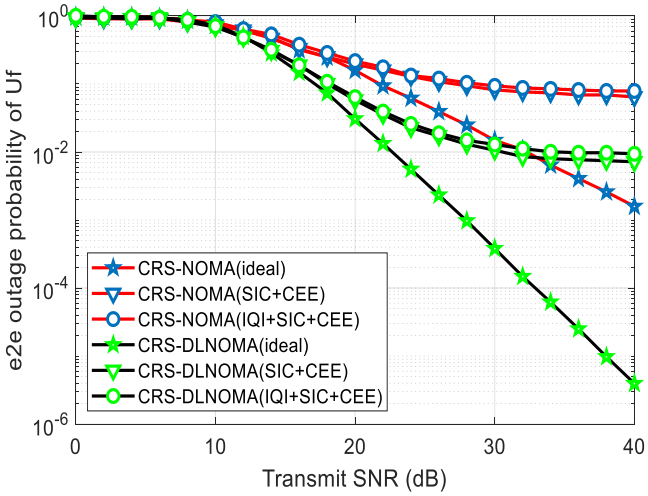

Fig. 2. Outage probability of (U_f) versus transmit SNR under CRS-NOMA and CRS-DLNOMA modes considering IQI factor ($k = 0.25$) and CEE ($\lambda_e = 0.008$)

In Fig. 2, the outage probability of U_f versus transmit SNR is plotted under CRS-NOMA and CRS-DLNOMA modes. We observe that in a perfect scenario, the outage probability of U_f decreases significantly, irrespective of the transmission mode of CNOMA. But, due to the availability of direct links and utilization of MRC at U_f, CRS-DLNOMA achieves better outage performance when SNR exceeds 25 dB. The results of the perfect scenario are also compared with the Outage performance of U_f considering IQI factor ($k = 0.25$), CEE ($\lambda_e = 0.008$), and SIC error ($\delta = 0.001$). Results show that all of these imperfections degrade the outage performance.

Additionally, compared to CEE and SIC errors, the IQI factor has less impact on the outage performance. Furthermore, CRS-DLNOMA with all imperfections achieves minimal outage probability compared to its counterpart, irrespective of the presence and absence of realistic imperfections when SNR<30 dB.

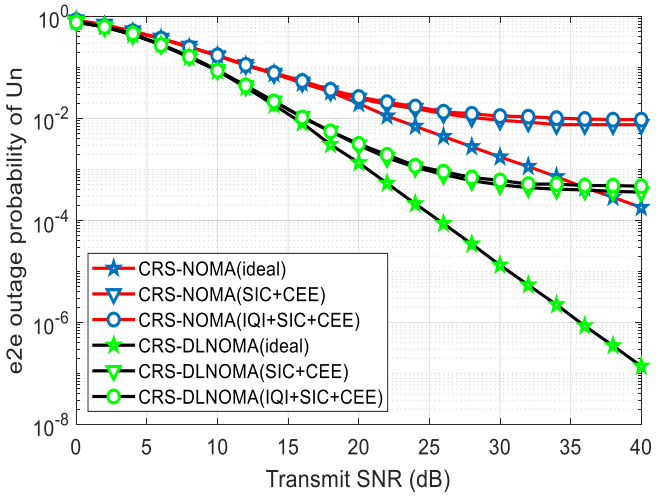

Fig. 3. Outage probability of (U_n) versus transmit SNR under CRS-NOMA and CRS-DLNOMA modes considering IQI factor ($k = 0.25$) and CEE ($\lambda_e = 0.008$)

The results of the outage probability of U_n versus transmit SNR are plotted under CRS-NOMA and CRS-DLNOMA modes in Fig. 3. The outcomes of the ideal case are also compared with the outage performance of U_n taking into account the IQI factor ($k = 0.25$), CEE ($\lambda_e = 0.008$), and SIC error ($\delta = 0.001$). Findings indicate that each of these flaws lowers the outage performance. The IQI component also has less effect on the outage performance than CEE and SIC errors. Additionally, when SNR is greater than 30 dB, CRS-DLNOMA with all flaws achieves the lowest outage probability compared to its equivalent, regardless of the presence or absence of actual imperfections. Furthermore, due to the utilization of MRC and cooperative transmission method, at 28 dB SNR U_n achieves a minimal outage probability of 0.000623 compared to U_f. Thus, with CRS-DLNOMA both U_n and U_f experience better transmission reliability even in the presence of realistic imperfections.

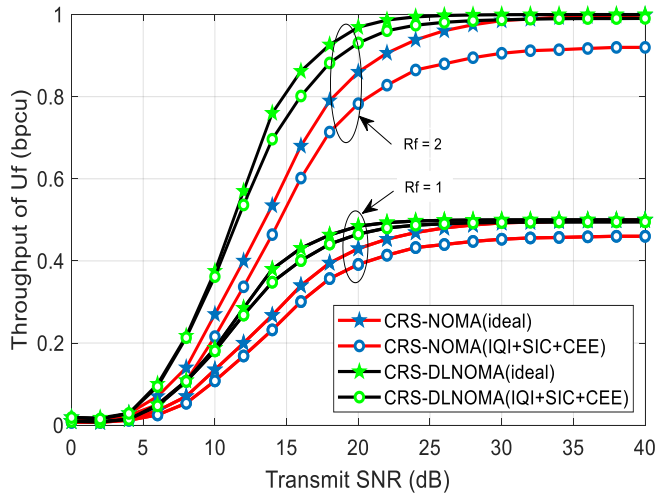

Fig. 4. Throughput of (U_f) versus Transmit SNR with IQI factor ($k = 0.25$) and CEE ($\lambda_e = 0.008$)

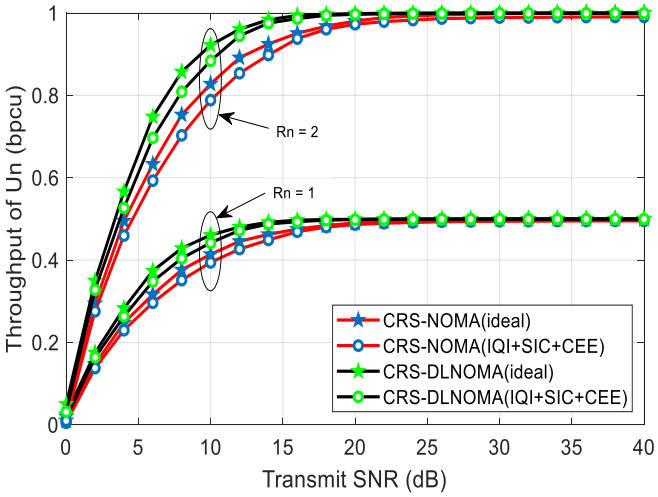

Fig. 5. Throughput of (U_n) versus transmit SNR with IQI factor ($k = 0.25$), and CEE ($\lambda_e = 0.008$)

The results of throughput versus transmit SNR are plotted in Fig. 4 and Fig. 5 for U_f and U_n respectively. In these simulations, we set desired transmission rates at users as $R_f = R_n = 1, 2$, IQI factor ($k = 0.25$) and CEE ($\lambda_e = 0.008$). Here we can observe that the simulation results match the closed-form throughput expressions of CRS-NOMA and CRS-DLNOMA modes obtained in (23) and (26), respectively. Results indicate that in all scenarios, the CRS-DLNOMA mode outperforms CRS-NOMA -based transmission because of the transmission diversity of the former scheme. On the other hand, in the presence of IQI and CEE, the throughput performance degrades for both transmission modes. By comparing the throughput performance of U_f with U_n, we observe that due to the utilization of MRC and cooperative transmission method, U_n achieved slightly higher throughput compared to U_f at medium and high SNR values for both transmission modes.

The impact of the IQI, SIC and CEE error on the overall system throughput for CRS-NOMA and CRS-DLNOMA modes is presented in Fig. 6. The results of overall throughput are plotted by setting desired transmission rates at users as $R_f = R_n = 1, 2$. It is observed that, for high SNR value, the

overall throughput is superior for both transmission modes. On the other hand, in the presence of all realistic impairments, CRS-DLNOMA achieves a maximum throughput of 0.986 bpcu compared to 0.925 bpcu attained for CRS-NOMA in the medium SNR range (10 dB to 25 dB). In addition, there is high distortion noise at the receiver for IQI factor greater than 0.2; CRS-DLNOMA mode is more beneficial than CRS-NOMA.

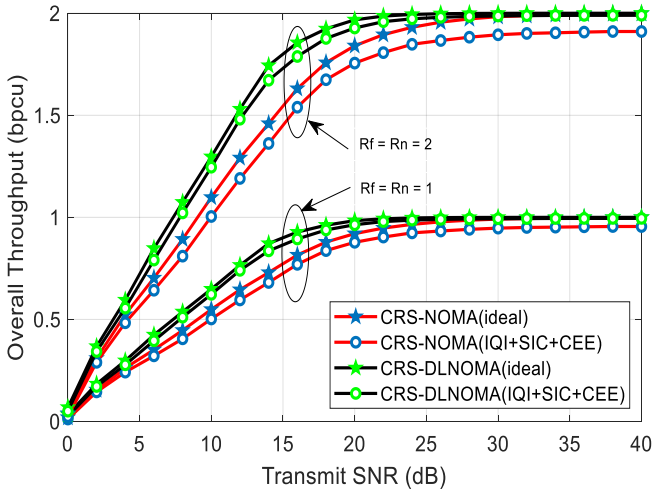

Fig. 6. System throughput versus transmit SNR considering ideal and realistic impairment scenario

In Fig. 7, the optimal throughput of U_n and U_f is plotted vs μ_n considering $R_f = R_n = 1.5$. It is observed that the throughput of U_n is an increasing function of μ_n initially and attains its maximum value of 0.748 bpcu at $\mu_n^{opt} = 1.5$, then decreases to 0 due to degradation in SINR value corresponding to the far user. In comparison to U_n, throughput of U_f continuously decreases with an increase in μ_n, so an optimal PAF is chosen to maximize the throughput performance of μ_n, while ensuring the throughput constraint at U_f. Additionally, due to the presence of a direct link, CRS-DLNOMA achieves significantly higher throughput compared to CRS-NOMA.

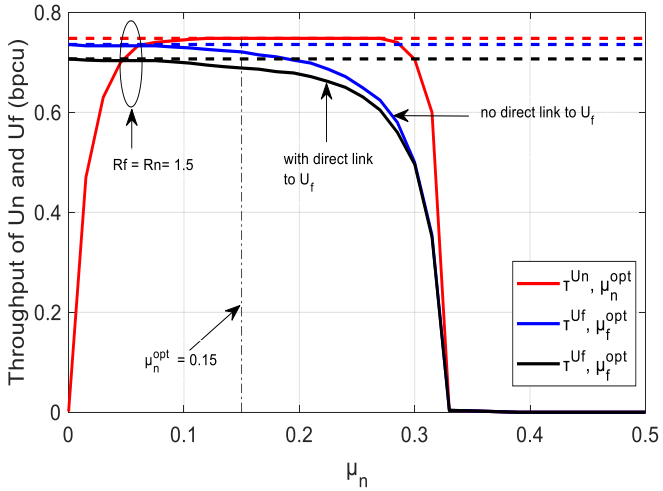

Fig. 7. Optimal throughput of U_n and U_f versus μ_n considering $R_f = R_n = 1.5$.

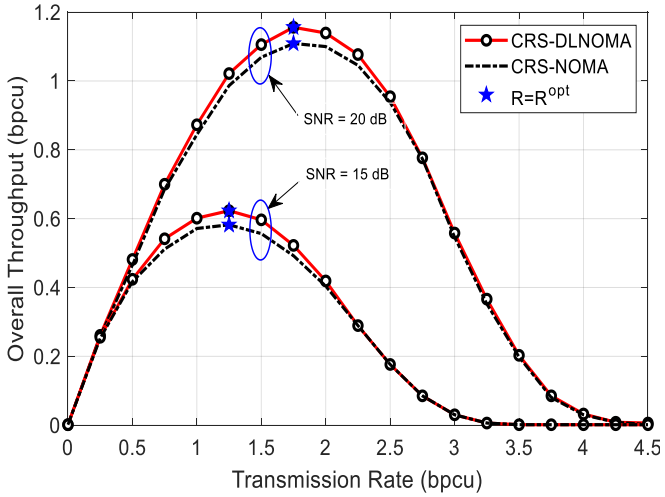

Fig. 8. Optimal system throughput versus $R(bpcu)$ considering SNR = 15, 20 dB.

The result of an optimal system throughput versus R (considering SNR = 15, 20 dB) is plotted in Fig. 8 for both CRS-NOMA and CRS-DLNOMA modes of transmission. As system throughput is concave w.r.t. R, it increases with an increase in R and achieves its maximum value when an optimal value of rate (R^{opt}) is selected. It is also evident from the result that the system throughput is superior for both transmission modes for higher SNR value. Moreover, because of the transmission diversity, CRS-DLNOMA achieves a significantly higher throughput of 1.156 bpcu (for $R^{opt} = 1.75$) and 0.6232 bpcu (for $R^{opt} = 1.25$) at 20 dB and 15 dB SNR, respectively.

7. Conclusions

This work investigates a NOMA-assisted cooperative relay system, where realistic impairments of IQI, CEE, and SIC error are considered. To analyze the effect of impairments, we derived analytical expressions of outage probability and throughput of near and far NOMA destinations. This analysis is also extended for the CNOMA model with two different modes of transmission: (i) Cooperative transmission without a direct link (CRS-NOMA) and (ii) Cooperative transmission with a direct link (CRS-DLNOMA). In a perfect scenario, the outage probability of U_f and U_n decreases significantly, irrespective of the transmission mode of CNOMA. But, due to the availability of direct links and utilization of MRC, CRS-DLNOMA achieves better outage performance when SNR is greater than 25 dB. Furthermore, due to the utilization of MRC and cooperative transmission method, at 28 dB SNR U_n achieves a minimal outage probability of 0.000623 compared to U_f. Throughput results indicate that in all scenarios, the CRS-DLNOMA mode outperforms CRS-NOMA-based transmission because of the transmission diversity of the former scheme. On the other hand, when IQI is increased beyond 0.18, the performance of both the user degrades irrespective of the transmission mode. Also, there is high distortion noise at the receiver for IQI factor greater than 0.2; CRS-DLNOMA is more beneficial than the CRS-NOMA transmission mode. Additionally, an efficient golden search-based algorithm was

also designed to optimize the PAF and transmission rate. The optimal values of PAF and rate were utilized to maximize the overall system throughput performance.

Statement of conflict of interest

On behalf of all authors, the corresponding author states that there is no conflict of interest.

References

[1] S. M. R. Islam, N. Avazov, O. A. Dobre, and K. S. Kwak, "Power-Domain Non-Orthogonal Multiple Access (NOMA) in 5G Systems: Potentials and Challenges," *IEEE Communications Surveys and Tutorials*, 2017, doi: 10.1109/COMST.2016.2621116.

[2] Tregancini, E. E. B. Olivo, D. P. M. Osorio, C. H. M. De Lima, and H. Alves, "Performance analysis of full-duplex relay-aided NOMA systems using partial relay selection," *IEEE Trans Veh Technol*, vol. 69, no. 1, pp. 622–635, Jan. 2020, doi: 10.1109/TVT.2019.2952526.

[3] J. Bae and Y. Han, "Joint Power and Time Allocation for Two-Way Cooperative NOMA," *IEEE Trans Veh Technol*, vol. 68, no. 12, pp. 12443–12447, Dec. 2019, doi: 10.1109/TVT.2019.2949129.

[4] K. Srinivasarao, P. Sharma, and M. Surendar, "Outage analysis for user selection based downlink cooperative NOMA network over generalized fading channels," *Digit Signal Process*, vol. 132, p. 103801, Dec. 2022, doi: 10.1016/J.DSP.2022.103801.

[5] L. Ma, E. Li, Q. Yang, X. Wang, and C. Song, "Performance Analysis and Optimization in Two-Way Cooperative NOMA Under Two-Phase Transmission Protocol," *IEEE Syst J*, vol. 16, no. 3, pp. 3566–3577, Sep. 2022, doi: 10.1109/JSYST.2022.3178074.

[6] L. Lv, Q. Ye, Z. Ding, Z. Li, N. Al-Dhahir, and J. Chen, "Multi-Antenna Two-Way Relay Based Cooperative NOMA," *IEEE Trans Wirel Commun*, vol. 19, no. 10, pp. 6486–6503, Oct. 2020, doi: 10.1109/TWC.2020.3003615.

[7] X. Li, M. Liu, C. Deng, P. Takis Mathiopoulos, Z. Ding, and Y. Liu, "Full-Duplex Cooperative NOMA Relaying Systems with I/Q Imbalance and Imperfect SIC," *IEEE Wireless Communications Letters*, vol. 9, no. 1, pp. 17–20, Jan. 2020, doi: 10.1109/LWC.2019.2939309.

[8] X. Liang, Y. Wu, D. W. K. Ng, S. Jin, Y. Yao, and T. Hong, "Outage Probability of Cooperative NOMA Networks under Imperfect CSI with User Selection," *IEEE Access*, vol. 8, pp. 117921–117931, 2020, doi: 10.1109/ACCESS.2020.2995875.

[9] X. Li, J. Li, Y. Liu, Z. Ding, and A. Nallanathan, "Residual Transceiver Hardware Impairments on Cooperative NOMA Networks," *IEEE Trans Wirel Commun*, vol. 19, no. 1, pp. 680–695, Jan. 2020, doi: 10.1109/TWC.2019.2947670.

[10] P. Bachan, A. Shukla, and A. Bansal, "Analysis of Erroneous SIC and CSI on the Outage Performance of Cooperative NOMA Systems," *Lecture Notes in Electrical Engineering*, vol. 877, pp. 569–577, 2023, doi: 10.1007/978-981-19-0312-0_56.

[11] O. Abbasi, A. Ebrahimi, and N. Mokari, "NOMA inspired cooperative relaying system using an AF relay," *IEEE Wireless Communications Letters*, vol. 8, no. 1, pp. 261–264, Feb. 2019, doi: 10.1109/LWC.2018.2869592.

[12] M. Aldababsa and O. Kucur, "Majority based antenna selection schemes in downlink NOMA network with channel estimation errors and feedback delay," *IET Communications*, vol. 14, no. 17, pp. 2931–2943, Oct. 2020, doi: 10.1049/IET-COM.2019.0937.

[13] S. Arzykulov, G. Nauryzbayev, A. Celik, and A. M. Eltawil, "Hardware and Interference Limited Cooperative CR-NOMA Networks under Imperfect SIC and CSI," *IEEE Open Journal of the Communications Society*, vol. 2, pp. 1473–1485, 2021, doi: 10.1109/OJCOMS.2021.3091606.

[14] D. Tweed, M. Derakhshani, S. Parsaeefard, and T. Le-Ngoc, "Outage-Constrained Resource Allocation in Uplink NOMA for Critical Applications," *IEEE Access*, vol. 5, pp. 27636–27648, Nov. 2017, doi: 10.1109/ACCESS.2017.2777601.

[15] S. Singh and M. Bansal, "Performance Analysis of NOMA-Based AF Cooperative Overlay System with Imperfect CSI and SIC," *IEEE Access*, vol. 9, pp. 40263–40273, 2021, doi: 10.1109/ACCESS.2021.3064177.

[16] P. Bachan, "SIC Error Impaired Cooperative NOMA-IoT Network: Throughput and Goodput Analysis," *2022 International Conference on Industry 4.0 Technology, I4Tech 2022*, 2022, doi: 10.1109/I4TECH55392.2022.9952530.

[17] S. Soni, R. Makkar, D. Rawal, and N. Sharma, "Performance Analysis of Selective DF Cooperative NOMA in Presence of Practical Impairments," *IEEE Syst J*, pp. 1–10, 2023, doi: 10.1109/JSYST.2023.3246996.

[18] T. E. A. Alharbi and D. K. C. So, "Full-Duplex Decode-and-Forward Cooperative Non-Orthogonal Multiple Access," *IEEE Vehicular Technology Conference*, vol. 2018-June, pp. 1–6, Jul. 2018, doi: 10.1109/VTCSPRING.2018.8417519.

[19] S. Mirabbasi and K. Martin, "Classical and modern receiver architectures," *IEEE Communications Magazine*, vol. 38, no. 11, pp. 132–139, Nov. 2000, doi: 10.1109/35.883502.

[20] Ö. Özdemir, R. Hamila, and N. Al-Dhahir, "I/Q imbalance in multiple beamforming {OFDM} transceivers: SINR analysis and digital baseband compensation," *IEEE Transactions on Communications*, vol. 61, no. 5, pp. 1914-1925, 2013.
doi: 10.1109/TCOMM.2013.021913.120321.

[21] Mohammadian and C. Tellambura, "RF Impairments in Wireless Transceivers: Phase Noise, CFO, and IQ Imbalance - A Survey," *IEEE Access*, vol. 9, pp. 111718–111791, 2021, doi: 10.1109/ACCESS.2021.3101845.

[22] B. Selim *et al.*, "Outage probability of multicarrier NOMA systems under joint I/Q imbalance," *Proceedings -2018 International Conference on Advanced Communication Technologies and Networking, CommNet 2018*, pp. 1–7, May 2018.
doi: 10.1109/COMMNET.2018.8360283.

[23] X. Li, M. Liu, D. Deng, J. Li, C. Deng, and Q. Yu, "Power beacon assisted wireless power cooperative relaying using NOMA with hardware impairments and imperfect CSI," *AEU - International Journal of Electronics and Communications*, vol. 108, pp. 275–286, Aug. 2019, doi: 10.1016/j.aeue.2019.06.034.

[24] D. Cui, X. Li, G. Huang, K. Rabie, G. Nauryzbayev, and B. M. El Halawany, "Outage Probability of ABCom NOMA Systems for 6G with IQI and RHIs," in *2022 13th International Symposium on Communication Systems, Networks and Digital Signal Processing, CSNDSP 2022*, Institute of Electrical and Electronics Engineers Inc., 2022, pp. 384–389.
doi: 10.1109/CSNDSP54353.2022.9908030.

[25] B. Selim, S. Muhaidat, P. C. Sofotasios, A. Al-Dweik, B. S. Sharif, and T. Stouraitis, "Radio-Frequency Front-End Impairments: Performance Degradation in Non-orthogonal Multiple Access Communication Systems," *IEEE Vehicular Technology Magazine*, vol. 14, no. 1, pp. 89–97, Mar. 2019, doi: 10.1109/MVT.2018.2867646.

[26] M. M. Alsmadi, N. A. Ali, M. Hayajneh, and S. S. Ikki, "Down-link NOMA networks in the presence of IQI and imperfect SIC: Receiver design and performance analysis," *IEEE Trans Veh Technol*, vol. 69, no. 6, pp. 6793–6797, Jun. 2020, doi: 10.1109/TVT.2020.2982171.

Received 18 June 2023